BJES Basrah Journal for Engineering Sciences

Basrah Journal for Engineering Sciences, Vol. 25, No. 2, (2025), 83-90

Original Article

Journal homepage: https://bjes.edu.iq/bjes
ISSN (Online): 23118385, ISSN (Print): 18146120

Numerical Failure Pressure Predication of Corrosion Defect in Transmission Pipeline

Nathera A. Saleh [1]*, Asaad K. Kadhim [2], Ayat I. Ali [3], Abdulrahman A. Adnan [4]

[1,2,3,4] *Mechanical Engineering Department, College of Engineering, University of Basrah, Basrah, Iraq*
E-mail addresses: nathera.saleh@uobasrah.edu.iq

Article Info

Article history:
Received: 30 July 2025
Revised:31 August 2025
Accepted: 22 September 2025
Published: 31 December 2025

Keywords:
Corrosion defect,
Finite element method,
Pressure predication.

https://doi.org/10.33971/bjes.25.2.9

Abstract

This study focuses on evaluating the structural integrity of SA-312 Grade TP316 pipeline with various forms of corrosion defects. The corrosion defects were characterized by three distinct geometries: internal rectangular, external rectangular, and internal elliptical. The effect of defect length, width and depth on pipeline failure pressure is investigated using the finite element method ANSYS software version 21. Regression analysis is conducted to develop equations relating maximum pressure to defect dimensions. The results show good agreement between the finite element results, experimental data, theoretical predictions, and design codes, with an error rate ranging from 3.98% to 17.79%. Failure pressure was found to be highly sensitive to corrosion dimensions, but the depth of corrosion has a greater impact on the failure pressure. Furthermore, it was observed that internal corrosion poses a greater threat to pipeline integrity than external corrosion.

1. Introduction

Pipelines are widely used to transport gas, oil, and other fluids over long distances. Therefore, they are considered effective components in many waters and energy transportation substructure. Though, over time, these components can wear out and weaken, mainly due to corrosion, which remains a very serious and influential problem that directly impacts the effectiveness of transmission pipelines. To avoid unforeseen failure, corrosion must be detected and treated, thus preserving equipment and reducing economic losses.

Essential importance in assessing the safety of pipelines is predicting the burst pressure, which is the maximum pressure a pipeline can withstand before bursting. Several techniques have been used to calculate this pressure, including empirical models such as the ASME B31G, RSTRENG, and DNV RP-F101[1]-[5], experimental procedures and numerical methods. Although empirical models provide practical guidance, they typically address corrosion cases of limited and simple forms. Corrosion engineering is known to encompass more complex cases. Furthermore, experimental tests are often expensive and potentially hazardous due to the high-pressure explosion of pipes. Numerical methods are therefore used to address more complex, less costly, and more safe cases. One such method is the finite element method, which is an effective tool for modeling the corrosion zone in pipes. It provides a clear view of the stress and strain distribution around the corroded areas, leading to more realistic failure pressure predictions [6], [7]. Therefore, the main objective of this research is to use the finite element method for various corrosion cases and compare the results with experimental data and available empirical models.

Based on the finite element method, many studies have investigated the prediction of failure pressure and evaluation of residual strength of corroded pipes by means of commercial FEM software such as ANSYS and ABAQUS. The results of these studies were compared by experimental data and additional calculation approaches to confirm the reliability and accuracy of the FEM simulation. It also allows the inclusion of important influences into the simulation that are often absent from empirical models, such as material plasticity, loading history and strain-hardening behavior, this adds an improvement to the accuracy of failure pressure calculation [6]-[9]. Gao et al [10] developed analytical methods of pipelines with long corrosion defects based on Tresca and von Mises criteria connected with deformation theory of plasticity under internal pressure and axial compressive stress. The validation of proposed model illustrations good agreement with finite element analysis and full-scale burst tests. Moreover, several studies integrated the finite element method with artificial neural networks to obvious empirical formula. Kumar et al. [11] presented a beneficial study on reviewing these studies and how can be combined or used these methods to expect the burst pressure of corroded pipelines, thus offering a powerful and effectual approach to pipeline integrity assessment. Zhang et al. [12] employed extended Finite Element Method (XFEM) to investigate the effect of crack depth on burst pressure of pipelines with crack in corrosion. Recently, Zhiwei et al. [13] investigated multiple pipeline grades API X52, X65, and X80 with varying defect depths to develop a predictive model (back-propagation neural network) to support integrity management based on FEA generated datasets.

From previous studies the geometric parameters of corrosion have been explored which are depth, length, and angle separately or two of them together. Where the study of corrosion depth is directly related to the remaining wall thickness of the pipe. Which in turn is considered one of the important factors in calculating the failure pressure. As for the length of corrosion length describes the extent of defect enlargement in the longitudinal direction, while corrosion angle represents the circumferential growth of a defect, which may affect stress distribution and consequently, failure style. Thus, this research investigates the effect of corrosion dimensions (i.e., depth, length and angle) together on failure pressure for various corrosion cases such as internal and external rectangular corrosion as well as elliptical corrosion. To improve the understand of corroded pipes behavior and thus develop better prediction models to support maintenance strategies.

2. Finite element modeling

2.1. Pipe geometry

The execution of present study was based on finite element analyses of SA-312 Grade TP316 pipeline with outer diameter (D: 168.3 mm), wall thickness (t: 7.11 mm), an ultimate strength of 530 MPa, a yield strength of 250 MPa and a modulus of elasticity of 193GPa.There are many applications that use this type of austenitic steel such as petroleum and chemical equipment, Heat exchangers, chemical transportation, and many others. The geometry of corroded pipes was generated using SolidWorks software to export it as IGES format for ANSYS software ver. 21. Because, in real cases corrosion defects have irregular and different shapes an idealization is required to represent the corrosion defect. Therefore, it was assumed that the corrosion defects have regular shape of internal rectangular, external rectangular and internal elliptical in this study [10], [11]. Eighty-one models were generated to represent all the cases studied, with twenty-seven models for each type of corrosion. Figure 1 shows the geometry of corroded pipe. Table 1 shows the dimensions of corrosion defects which are depth (d), length (L) and angle (β).

Table 1. Dimensions of corrosion defects

Depth (d) (mm)	Angle (β) (rad)	Length (L) (mm)
1.185	0.349	51.36
2.37	0.698	102.72
3.555	1.0472	154.08

2.2. Meshing

The mesh generated was a tetrahedral-shaped mesh with sufficient refinement prepared at the corrosion defects of 3mm element size. The element size was chosen after several attempts and this size was the most appropriate when comparing the results. Gradually the element size of the uncorroded region was increased when transitioning away from the corrosion defects as demonstrated in Fig. 2, to reduce simulation time without losing solution accuracy

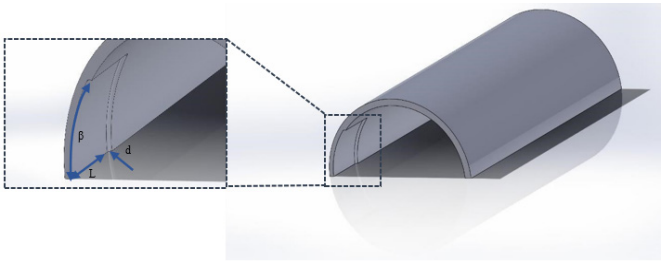

(a) internal rectangular.

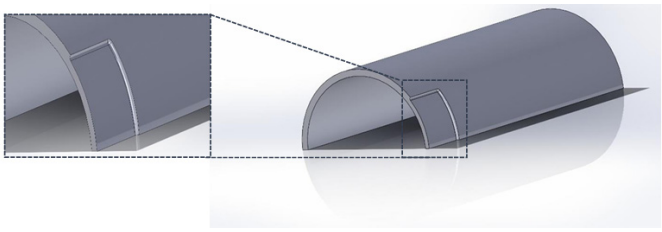

(b) external rectangular.

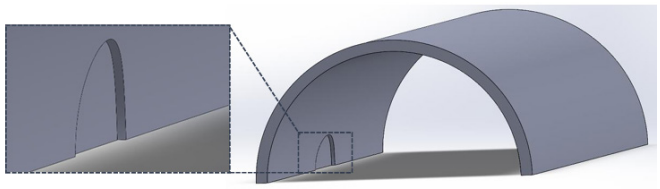

(c) internal elliptical

Fig. 1 Geometry of corroded pipe.

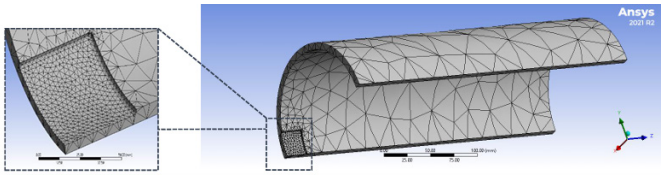

Fig. 2 Meshing of corroded pipe

2.3. Load and boundary conditions

A corroded pipe may be exposed to more than one load at once, such as tension and compression, as in the case of buried pipes due to soil movement or to an external load due to the fluid surrounding of offshore pipeline. The operating condition considering in this study is internal pressure only on all of the internal surfaces of the pipe. Based on failure criteria that the burst pressure can be obtained when the von-Mises stress reaches the ultimate tensile strength of the material of the pipe, thus the internal pressure has been increased gradually until reached this value [14].

As much as possible, symmetric boundary conditions are executed, and thus it is possible to build a half or a quarter model to reduce the calculation execution time. Figure 3 shows the boundary conditions of all considered case studies. Where, the end nodes were considered as constrain in the longitudinal and angular directions to simulate the effect of end caps.

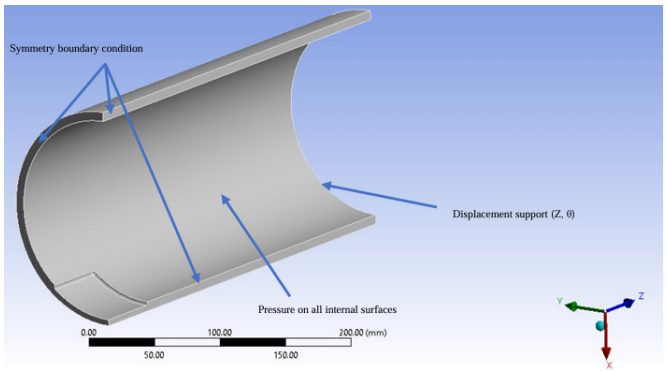

(a) Boundary conditions for rectangular corrosion (inner and outer).

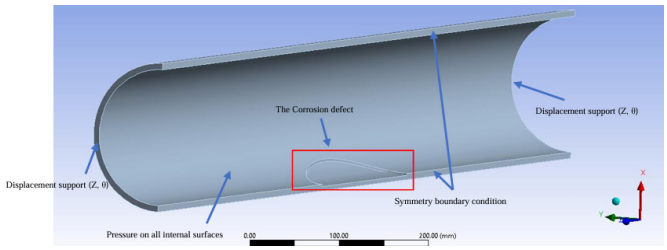

(b) Boundary conditions for elliptical corrosion.

Fig. 3 Boundary conditions for case studies.

2.4. Validation of finite element model

To verify the validity of the results, the finite element method results were compared with different cases of published studies based on practical tests or theoretical model, as shown in Table 2. From this table, the highest error which was 14.37%, with practical tests, because this depends on the test conditions. Also, can be noted that when comparing with Gao et al. [10], where they used a theoretical model based on failure theories (i.e., Tresca criterion and Von Mises criterion), the error was greater with the Tresca model than the Von Mises model. In this study, an equation has been developed to calculates the burst pressure for long pipelines (where the defect length is longer than $\sqrt{20Dt}$ as recommended because if the corrosion length is higher than this value then it has very little effect on the burst pressure of the pipeline [1].

The results were also compared with the most important approved engineering specifications. Table 3 displays the error between the FEM results of all case studies of internal rectangular defects and different semi-empirical equations. It is worth noting that ASME B31G-2009 [1] and Cosham et al. [5] depend on the effect of corrosion length and depth besides used failure theories, while Kastner et al. [18] relied on the effect of corrosion angle and depth, whereas the current study took length, depth, and angle into account. Therefore, there is a difference in failure pressure values as noted in Table 3.

Table 2. Validation of finite element model.

Description of tested pipe	Burst Pressure of published studies (MPa)	Predicted pressure (FEM) (MPa)	Error %
Zhu and Leis [15], without a corrosion defect exp. work	36.33	37.898	4.3
Abdelghani et al. [16], with internal corrosion defect exp. work	9.13	7.828	14.26
Kim et al. [17], with external corrosion defect exp. work	19.1	16.7	14.37
Gao et al. [10], theoretical model (Tresca criterion)	30.538	35.35	15.76
Gao et al. [10], theoretical model (Von Mises criterion)	36.817	35.35	3.98

Table 3. Comparison between the FEM and semi-empirical equations

Assessment method	Error %
ASME B31G-2009 [1]	17.79
Cosham et al. [5]	7.34
Kastner et al. [18]	4.25

For the benefit, below is a list of assessment equations that were used to compare. And Table 4 shows the denotation of each symbol in the failure pressure model equations.

ASME B31G-2009 [1]

$$P_f = \frac{2(1.1\sigma_y + 68.95)t}{D}\left(\frac{1-0.85\frac{d}{t}}{1-0.85\frac{d}{t}M1^{-1}}\right) \quad (1)$$

$$M1 = 0.032\frac{L}{(Dt)^{1/2}} + 3.3 \qquad if \quad \frac{L}{(Dt)^{1/2}} > 50$$

$$M1 = \left(1 + 0.6275\left(\frac{L}{(Dt)^{1/2}}\right) - 0.003375\left(\frac{L}{(Dt)^{1/2}}\right)^2\right)^{\frac{1}{2}} \qquad if \quad \frac{L}{(Dt)^{1/2}} < 50$$

Cosham et al. [5]

$$P_f = \frac{2(\sigma_y + 68.95)t}{D}\left(\frac{1-0.85\frac{d}{t}}{1-0.85\frac{d}{t}M1^{-1}}\right) \quad (2)$$

Gao et al. [10]:

$$P_f = k^{n+1}\left(\frac{e}{n}\right)^n \sigma_u' \frac{2t_0}{D_0 - 2t_0}\left(1 - \frac{d_0}{t_0}\right)\frac{(lna)^n}{a - a\beta + a^2\beta} \quad (3)$$

$$a = \frac{(1 + 1.404\beta)e^n - 1.515n\beta}{1 + 1.38139\beta}$$

$k = 1$ *(Von Mises criterion)*

$k = 2/\sqrt{3}$ *(Tresca criterion)*

Kastner et al. [18]

$$P_f = \frac{2t\sigma_{axial}}{D} \quad (4)$$

$$\sigma_{axial} = \sigma_{flow}\frac{\left(1-\frac{d}{t}\right)\left\{\pi-\beta\left[1-\left(1-\frac{d}{t}\right)\right]\right\}}{\left(1-\frac{d}{t}\right)\pi+2\left[1-\left(1-\frac{d}{t}\right)\right]sin(\beta)}$$

Table 4. terms of the Failure pressure model equations.

Symbol	Definition	Symbol	Definition
β	Half defect angle (radian)	t	Thickness of the pipe
d	Defect depth	η = 1- d/t	Defect depth ratio
D	Outside diameter of the pipe (mm)	$p = \frac{PR}{t\sigma_f}$	Pressure parameter
L	Defect length	$\sigma_t = \frac{\sigma_u + \sigma_y}{2.4}$	Flow stress (MPa)
R	Outside radius	σ_u	Ultimate tensile stress (MPa)
σ_y	Yield stress	$P = PF = Pb$	Burst pressure
n	Strain hardening exponent	e	Natural constant equal to 2.7183

3. Results and discussion

As mentioned earlier, the case studies which studied are internal rectangular, external rectangular and internal elliptical. The input parameters for the corrosion defects are defined by the three dimensions: width (β), depth (d), and length (L) as exposed in table 1.

Stress analysis exposes that the defects cause a rise in stress concentration at the defect location, where the maximum von Mises stress is noticed. The stress gradually intensifies until it crests at the defect place which is region of smallest material thickness, demonstrating that failure starts from the site of corrosion. While it is more stable in areas far from corrosion. Figure 4 displays the contours stress distribution of von Mises equivalent of an internal rectangular corrosion defect.

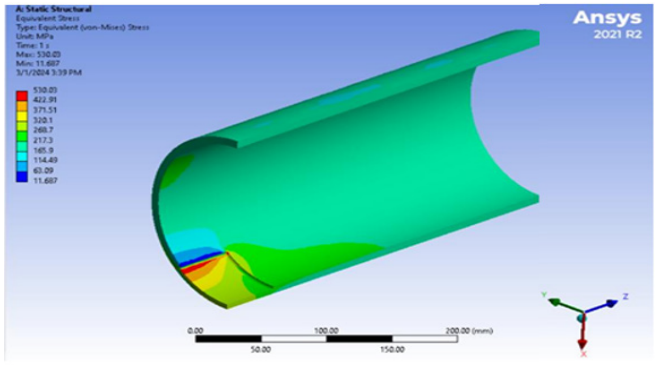

Fig. 4 Distribution of Von Mises stress around the defect for internal corrosion.

3.1. Internal and external rectangular corrosion

To represent the study cases of internal corrosion closer to reality, the rounding of the corners was used to reduce the concentration of stresses, and when compared with the theoretical equations mentioned earlier, the results were close. From the results can be observed that the burst pressure is decreased by 37.9% - 61.7% for considered case studies as compared with design pressure of this pipe which is 40 MPa [18]. In general, this shows a decrease in failure pressure as the corrosion dimensions increase. In order to investigate how the position of the corrosion defects whether internal or external effects the burst pressure, Fig. 5 was constructed.

The pressures were lower in the case of internal corrosion than external corrosion, sometimes they approaching. Thus, this shows that internal corrosion is more serious than external corrosion.

To clarify the relationship between corrosion defects parameters and failure pressure, mathematical equations were developed based on the regression analysis using MATLAB 2023b package. Two equations were generated the first one is a linear equation and the second one is a second-degree polynomial equation. All the equations generated were normalized to thickness (i.e., *d/t*, *β/t* and *L/t*). It's evident by the comparison with finite element method that the polynomial equation gives a better approximation than linear equation. Figure 6 illustrates the comparison between the finite element method and the two equations

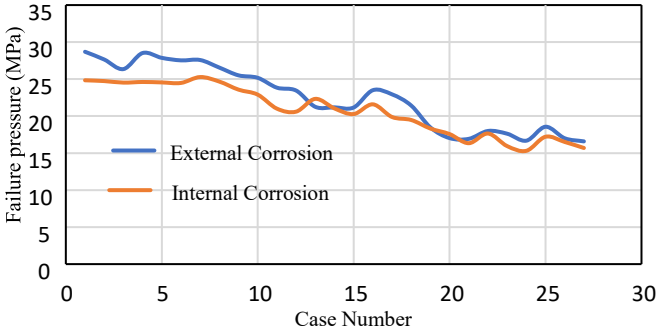

Fig. 5 Comparison between internal and external rectangular corrosion.

3.1.1. Internal corrosion

1. Linear equation with error of 2.75 %

$$P_f = 31.0087 - 23.5727\frac{d}{t} - 2.2987\beta - 0.05357\frac{L}{t} \quad (5)$$

2. Polynomial equation with error of 1.55 %

$$\begin{aligned} P_f = {} & 28.6335 - 0.1072\frac{L}{t} - 1.1718\beta - 9.1706\frac{d}{t} \\ & - 0.0246\frac{L}{t}\beta - 0.2555\frac{d}{t}\frac{L}{t} - 3.191\beta\frac{d}{t} \\ & + 0.0034\left(\frac{L}{t}\right)^2 + 1.0618\beta^2 \\ & - 12.7281\left(\frac{d}{t}\right)^2 \end{aligned} \quad (6)$$

3.1.2. External corrosion

1. Linear equation with error of 2.69 %

$$P_f = 34.8648 - 29.797\frac{d}{t} - 1.2632\beta - 0.1086\frac{L}{t} \quad (7)$$

2. Polynomial equation with error of 2.46 %

$$P_f = 36.7136 - 0.1712\frac{L}{t} - 7.1892\beta - 26.8443\frac{d}{t} - 0.0171\frac{L}{t}\beta - 0.0395\frac{L}{t}\frac{d}{t} - 3.985\beta\frac{d}{t} + 0.0021\left(\frac{L}{t}\right)^2 + 3.4697\beta^2 - 9.4623\left(\frac{d}{t}\right)^2 \quad (8)$$

3.2. Internal elliptical corrosion

The elliptical corrosion was chosen because it is closer to realistic situations than the rectangular shape, and also because the absence of an angle means less stress concentration. Additionally, there was no semi-empirical equations to calculate the failure pressure for this type of corrosion. It's clear that the rectangular corrosion has more uniform effect on the failure pressure than the elliptical corrosion, due to flow disturbances and variations in the corrosion elliptical area as revealed in Fig. 7.

For the elliptical corrosion a polynomial equation was generated and it gave an error of 3.4 %. Figure 8 shows the difference between this equation and the values acquired from the finite element method.

$$P_f = 24.9278 - 0.2871\frac{L}{t} - 14.86572\beta - 9.6013\frac{d}{t} - 0.0881\frac{L}{t}\beta - 0.3313\frac{L}{t}\frac{d}{t} - 9.6552\beta\frac{d}{t} + 0.0062\left(\frac{L}{t}\right)^2 + 3.5274\beta^2 - 14.0699\left(\frac{d}{t}\right)^2 \quad (9)$$

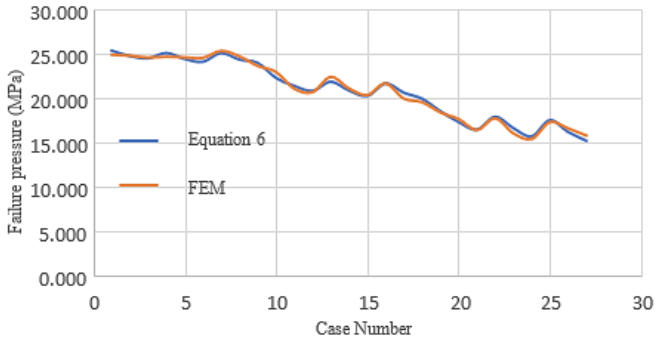

(a) internal rectangular corrosion.

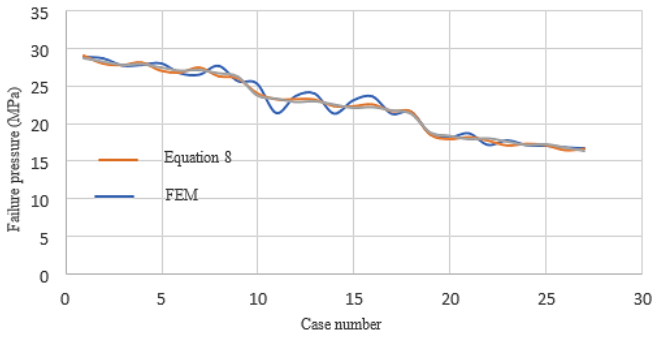

(b) external rectangular corrosion.

Fig. 6 FEM vs derived equations of failure pressure for internal and external rectangular corrosion.

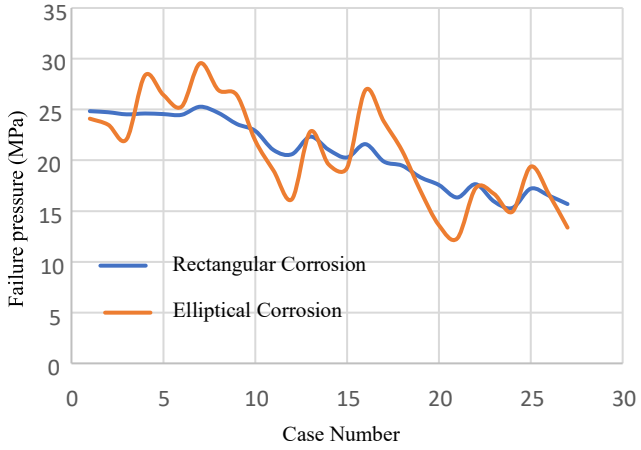

Fig. 7 Comparison between internal rectangular and elliptical of failure pressure.

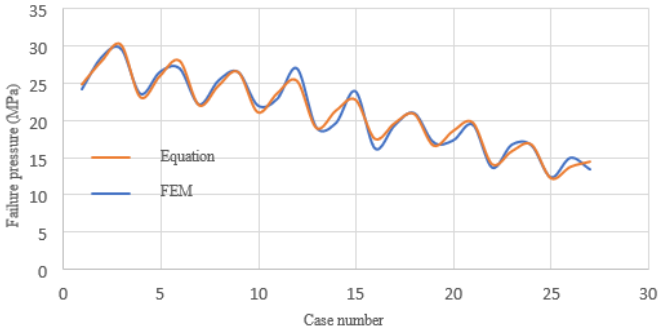

Fig. 8 FEM vs derived equations of failure pressure for internal elliptical corrosion.

3.3. Effect of corrosion parameters and types on failure pressure

The obtained results showed that corrosion depth has great effect on the failure pressure of the three types of corrosion as exposed in Figs. 9-11. This effect was due to the local thinning in the cross-section area and it's known that the failure pressure of any pipe depends directly on its thickness. It's noted that the decrease in failure pressure for varying corrosion depth $d = 1.185$, $d = 2.37$ and $d = 3.555$ are 37%, 42% and 54% respectively for constant length and angle. According to ASME B31G [1] the maximum acceptable corrosion depth can be calculated based on corrosion length and vice versa. Table 7 illustrations the maximum acceptable corrosion depth and length for the selected case studies. For further details, the appendix shows the corrosion dimensions and corresponding burst pressure values for all corrosion types.

Table 7. Acceptable corrosion depths and lengths used according to ASME B31G [1].

Corrosion length (mm) of current study	Acceptable depth (mm) according to ASME B31G [1]	Corrosion depth (mm) of current study	Acceptable length (mm) according to ASME B31G [1]
51.36	2.187	1.185	140.076
102.72	1.454	2.37	46.23
154.08	1.011	3.555	29.76

From previous illustrations and tables can be revealed that the most dangerous type of corrosion is internal rectangular corrosion. This is qualified to conditions that disturb or change the behavior of fluid flow over time, such as pressure drops and flow resistance or even diversion of flow. Due to varying pipe geometry, growing roughness, presenting debris, or leading to leaks. Whereas external rectangular corrosion is less dangerous despite having almost symmetrical stress concentration. While internal elliptical corrosion can be considered less dangerous compared to the two former kinds. This is credited to its lower stress concentration due to the absence of angles, which are one of the main causes of stress concentration. It is also worth observing that the dimensions used were the same for all types, but the elliptical is measured occupies less space (i.e., area) compared to the internal and external rectangles.

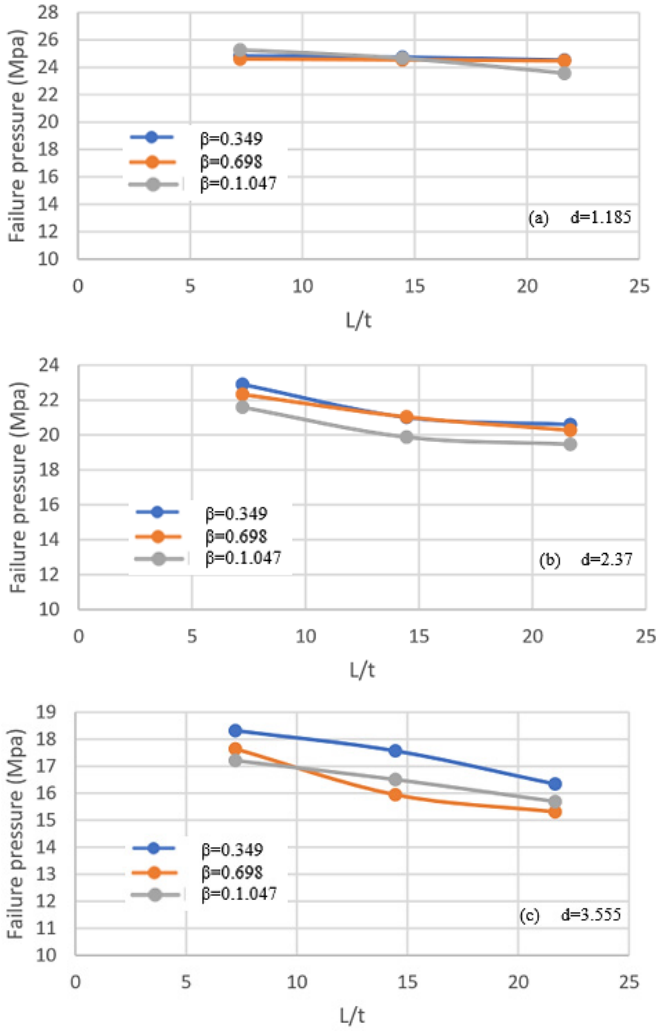

Fig. 9 Effect of corrosion parameters on the failure pressure (internal rectangular corrosion).

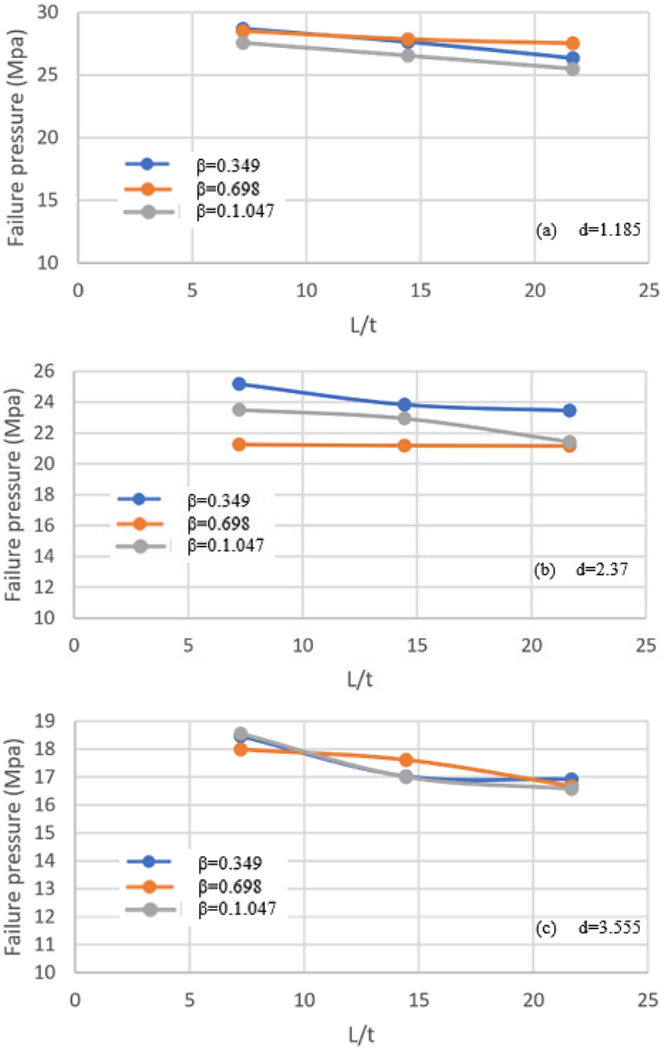

Fig. 10 Effect of corrosion parameters on the failure pressure (external rectangular corrosion).

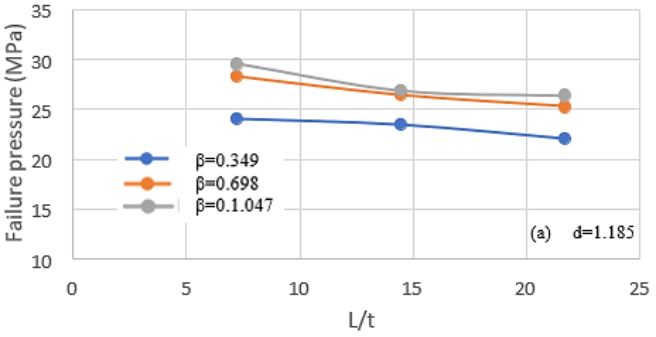

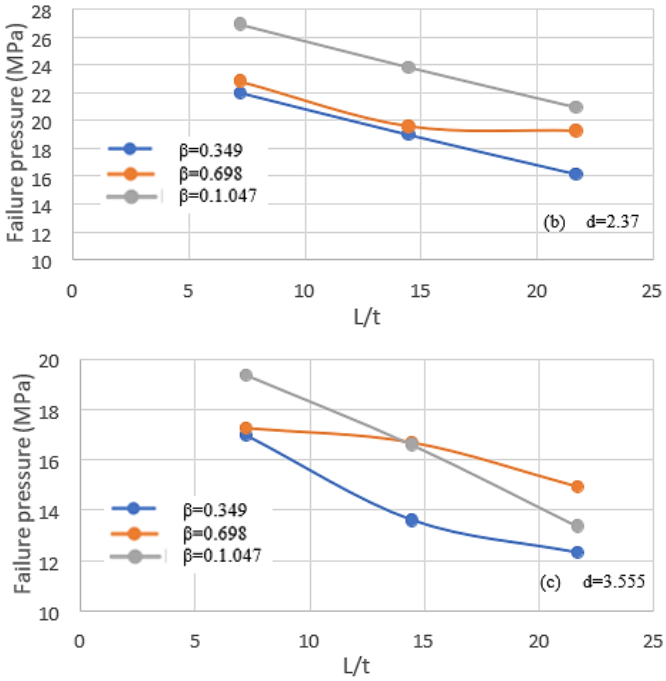

Fig. 11 Effect of corrosion parameters on the failure pressure (internal elliptical corrosion).

4. Conclusions

Based on the results of the study concerning the estimation of burst pressure using finite element method for three forms of corrosion defects internal rectangular corrosion, external rectangular corrosion, and internal elliptical corrosion, the following conclusions can be drawn:

1. The results establish a good agreement between the burst pressure estimated through FEM simulations and that obtained from previously published experimental and semi-empirical assessments with a maximum error of 17.79% for internal corrosion and 14.37% for external corrosion, this may be attributed to the fact that the corrosion taken by FEM is larger in size as it was approximated to a rectangle. While in the case of without corrosion the error was 4.31%. This recommends that FEM is a reliable method for predicting burst pressure in pipelines with various forms of corrosion defects.
2. The regression analysis evaluation formulas developed in the study reveals that these formulas are highly precise in estimating burst pressure. This suggests that the developed formulas can be effectively used as predictive tools for assessing the burst pressure of pipelines with corrosion defects.
3. The most influential dimension on the burst pressure is the depth that thin the thickness, as it greatly reduces the pressure up to 54%, followed by the length which has less impact than the depth but more than the angle (width), meaning that the angle (width) has the least impact among the dimensions.
4. Internal corrosion emerged as the most dangerous condition compared with external one, also the elliptical one less dangerous than the rectangular one.

Appendix

Appendix corrosion dimensions and corresponding burst pressure values for all corrosion types.

Case No.	*d* (mm)	*β* (Rad)	*L* (mm)	Burst Pressure (MPa)		
				rectangular		internal elliptical
				internal	external	
1	1.185	0.349	51.36	24.838	28.693	24.101
2	1.185	0.349	102.72	24.733	27.6460	23.500
3	1.185	0.349	154.08	24.525	26.3510	22.073
4	1.185	0.698	51.36	24.611	28.5200	28.356
5	1.185	0.698	102.72	24.549	27.8670	26.443
6	1.185	0.698	154.08	24.481	27.5300	25.295
7	1.185	1.047	51.36	25.273	27.5750	29.554
8	1.185	1.047	102.72	24.662	26.5530	26.908
9	1.185	1.047	154.08	23.574	25.5050	26.422
10	2.37	0.349	51.36	22.897	25.1720	21.945
11	2.37	0.349	102.72	21.007	23.8390	18.976
12	2.37	0.349	154.08	20.600	23.4530	16.172
13	2.37	0.698	51.36	22.327	21.2540	22.824
14	2.37	0.698	102.72	21.034	21.1820	19.585
15	2.37	0.698	154.08	20.274	21.1630	19.262
16	2.37	1.047	51.36	21.590	23.4980	26.915
17	2.37	1.047	102.72	19.878	22.9390	23.826
18	2.37	1.047	154.08	19.472	21.4230	20.924
19	3.555	0.349	51.36	18.317	18.4690	16.979
20	3.555	0.349	102.72	17.568	17.0260	13.606
21	3.555	0.349	154.08	16.337	16.9250	12.308
22	3.555	0.698	51.36	17.644	17.9890	17.260
23	3.555	0.698	102.72	15.946	17.6170	16.692
24	3.555	0.698	154.08	15.309	16.6790	14.936
25	3.555	1.047	51.36	17.209	18.5590	19.378
26	3.555	1.047	102.72	16.507	17.0030	16.611
27	3.555	1.047	154.08	15.691	16.5820	13.370

References

[1] American Society of Mechanical Engineers, B31.G-2012: Manual for Determining the Remaining Strength of Corroded Pipelines: Supplement to ASME B31 Code for Pressure Piping, ASME, 2012.

[2] J. F. Kiefner, P. H. Vieth, “A Modified Criterion for Evaluating the Remaining Strength of Corroded Pipe”, Final report on Project PR 3-805 to the Pipeline Research Committee of the American Gas Association, 1989.

[3] DNV. Recommended Practice DNV-RP-F101. Oslo, 2017.

[4] R. G. Amaya, M. S. Sánchez, A. E. Schoefs, F. F. Munoz, "Reliability assessments of corroded pipelines based on internal pressure, A review," Engineering Failure Analysis, Vol.98, pp.190-214, 2019. https://doi.org/10.1016/j.engfailanal.2019.01.064

[5] A. Cosham, P. Hopkins, K. A. Macdonald, "Best practice for the assessment of defects in pipelines Corrosion," Engineering Failure Analysis, Vol. 14, pp. 1245-1265, 2007. https://doi.org/10.1016/j.engfailanal.2006.11.035

[6] J. B. Choi, J. H. Kim, Y. H. Park, "Burst pressure evaluation of corroded gas pipelines using finite element analysis," International Journal of Pressure Vessels and Piping, Vol. 86, Issue 10, pp. 607-613, 2009. https://doi.org/10.1016/j.ijpvp.2009.06.002

[7] Z. Yang, D. Liu, X. Zhang, "Finite element method analysis of the stress for line pipe with corrode groove during outdoor storage," Acta Metall. Sinica (English Letters, Vol. 26, pp. 188-198, 2013. https://doi.org/10.1007/s40195-012-0122-4

[8] J. Zhou, L. Zhang, Y. Cheng, "Finite element modeling of the failure pressure of corroded pipelines," Corrosion Science, Vol. 87, pp.144-152, 2014. https://doi.org/10.1016/j.corsci.2014.06.034

[9] Y. Jiang, W. Zhao, X. Li, X. Zhang, "Failure pressure prediction of corroded pipeline based on finite element method," Engineering Failure Analysis, Vol. 68, pp. 76-85, 2016. https://doi.org/10.1016/j.engfailanal.2016.05.008

[10] J. Gao, P. Yang, L. Xin, J. Zhou, J. Liu "Analytical prediction of failure pressure for pipeline with long corrosion defect," Ocean Engineering, Vol. 191, pp. 106-497, 2019. https://doi.org/10.1016/j.oceaneng.2019.106497

[11] S. D. V. Kumar, M. Lo, T. Arumugam, S. Karuppanan, "A review of finite element analysis and artificial neural networks as failure pressure prediction tools for corroded pipelines", Materials, Vol. 14, Issue 6135, pp. 1-15, 2021. https://doi.org/10.3390/ma14206135

[12] X. Zhang, A. Okodi, L. Tan, J. Leung, S. Adeeb, "Failure Pressure Prediction of Cracks in Corrosion Defects Using XFEM X", Proceedings of the 2020 13th International Pipeline Conference, IPC 2020. https://doi.org/10.1115/IPC2020-9312,

[13] Z. H. Z. Huang, D. Wang, J. Han, "Study on Failure Pressure and Life Prediction of Defective Pipelines Based on Numerical Simulation", Journal of Computational Methods in Sciences and Engineering, Vol. 24, Issue 6, 2024. https://doi.org/10.1177/14727978241293275,

[14] J. B. Choi, B. K. Goo, J. C. Kim, Y. J. Kim, W. S. Kim, "Development of Limit Load Solutions for Corroded Gas Pipelines", International Journal of Pressure Vessels and Piping, Vol. 80, Issue 2, pp. 121-128, 2003. https://doi.org/10.1016/S0308-0161(03)00005-X

[15] X. K. Zhu, B. N. Leis, "Evaluation of burst pressure prediction models for line pipes", International Journal of Pressure Vessels and Piping, Vol. 89, pp. 85-97, 2012. https://doi.org/10.1016/j.ijpvp.2011.09.007

[16] M. Abdelghani, G. Tewfik, D. Djahida, S. S. Ahmed, "Prediction of the Rupture Pressure of Transmission Pipelines with Corrosion Defects," Journal of Pressure Vessel Technology, Vol. 140, Issue 4, 2018. https://doi.org/10.1115/1.4039698

[17] W. S. Kim, Y. P. Kim, Y. T. Kho, J.-B. Choi, "Full Scale Burst Test and Finite Element Analysis on Corroded Gas Pipeline," 4th International Pipeline Conference, Parts A and B, pp. 1501-1508, 2009. https://doi.org/10.1115/IPC2002-27037

[18] W. Kastner, E. Roehrich, W. Schmitt, R. Steinbuch, "Critical crack sizes in ductile piping", Int. J. Pres. Ves. and Piping, Vol.9, Issue 3, pp.197-219,1981. https://doi.org/10.1016/0308-0161(81)90002-8